3-D prestack migration: two implementations

John T. Etgen

ABSTRACT

Two techniques for prestack migration in two dimensions, the finite-difference reverse-time method and the Kirchhoff integral method, can be used for prestack migration in three dimensions. Because of the tremendous amount of data present in a 3-D survey, the migrations are posed as individual shot profile migrations. If the data for one field profile are collected on an x, y grid (areal data) then the reverse-time prestack migration is an appropriate method for 3-D prestack migration. This is most common for high-resolution 3-D land surveys. If the data for one field profile are collected only along a line, then the Kirchhoff integral method is appropriate. Non-uniform spatial sampling is more easily accommodated by the Kirchhoff integral method.

INTRODUCTION

Three-dimensional prestack migration is an expensive process, but may be necessary to provide an accurate image of three-dimensional subsurface structure. When the subsurface structure does not lend itself to the concepts of strike and dip, 2-D methods may not produce interpretable images of the subsurface. True 3-D processing is necessary. Prestack migration in three-dimensions can provide an accurate image of a complex, 3-D subsurface when other methods fail.

For two-dimensional surveys, trace sampling intervals and line length play important roles in the quality of a prestack migration. The effect of sampling intervals and line-length are even more important for 3-D prestack migration because cost constraints dictate sparse sampling. Many 3-D surveys are poorly sampled along one of the spatial axes; how a migration method handles this is important. Prestack interpolation of 3-D data, which is beyond the scope of this paper, may be necessary to overcome spatial aliasing.

Two types of three-dimensional surveys are considered and a prestack migration method is outlined for each. The first type of survey discussed has an areal grid (in x, y) of receivers for each shot. This is most common with high resolution land 3-D surveys. The second type of survey considered is more common in the marine environment. A ship (or ships) will collect a series of closely spaced lines. The resulting grid of traces comprises the 3-D survey. For any given shot, there is only one line of receivers or possibly two. For 3-D areal

data, each shot profile migration is an independent estimate of the underlying 3-D structure of the Earth because information about both x and y directions was recorded for each shot; thus, information about both the x and y directions is contained in the migration of each profile. It is possible that only a small number of migrated profiles will be needed to provide an image of the subsurface. For linear data, only one line or at most two lines are recorded for each shot profile; the data from one profile does not contain enough information about the cross-line direction to form an image of a 3-D subsurface. The inline direction is referred to as the x direction and the cross-line direction is referred to as the y direction. Moreover, little or no resolution is obtained in the y direction by migrating an individual line. Many parallel (or nearly parallel) lines are required to obtain resolution in the cross-line direction. If the cross-line spacing is large, only shallow dips can be resolved in that direction. The Kirchhoff integral method is able to deal with these restrictions in a more natural way than the finite-difference method.

FINITE-DIFFERENCE REVERSE-TIME PRESTACK MIGRATION

Prestack migration in three dimensions with a finite-difference reverse-time method is similar to the method applied in two dimensions (Etgen, 1986). The data is time-reversed and used as a boundary condition on the surface of a 3-D velocity model. The resulting wave field is allowed to propagate back into the model. A second-order in time, eighth-order in x, y, z finite-difference representation of equation (1), the 3-D acoustic wave equation is used to back-propagate the recorded wave field into the model (Etgen, 1986). The two-way non-reflecting wave equation is not used because a smooth velocity model is assumed.

$$\frac{\partial^2 U}{\partial t^2} = V^2(x,y,z) \cdot [\frac{\partial^2 U}{\partial x^2} + \frac{\partial^2 U}{\partial z^2} + \frac{\partial^2 U}{\partial y^2}] \tag{1}$$

The shot wave field is extrapolated from the shot point into the model using WKB ray theory. The traveltimes and amplitudes of the shot wave field are precomputed using the same methods as in the paper on fast prestack depth migration in this report (Etgen, 1987). It is possible to extrapolate the shot wave field using the same finite-difference method as used for the recorded wave field. However, propagating both the shot wave field and the recorded wave field will require twice as much core memory as extrapolating the shot wave field with ray theory. The recorded wave field, at a given time level, is imaged by the shot wave field by multiplying the amplitude of the shot wave field, at that time level, by the back-propagated recorded wave field, at the same time level. Partial images are built up for each time level as time runs backward, and added together to form the image of one profile. The results from the different profiles can be stacked to form the final image.

Absorbing boundaries are used on all sides and on the bottom of the model. Each absorbing boundary is an appropriate one-way, 15 degree equation. Adding only a few grid points around the model in all directions can increase the required storage and computation dramatically; so it would be impractical to use absorbing boundaries that require many points. The absorbing boundary must use as few points as possible, and still provide adequate absorption, so one-way equations are ideal. For the eighth-order spatial derivative finite-difference formulation, the absorbing boundaries are expressed over 4 points. The one-way equations used were not high-order equations in terms of either the dispersion relation or the order of the difference operators so the cost of computing the wave field in the boundary is insignificant.

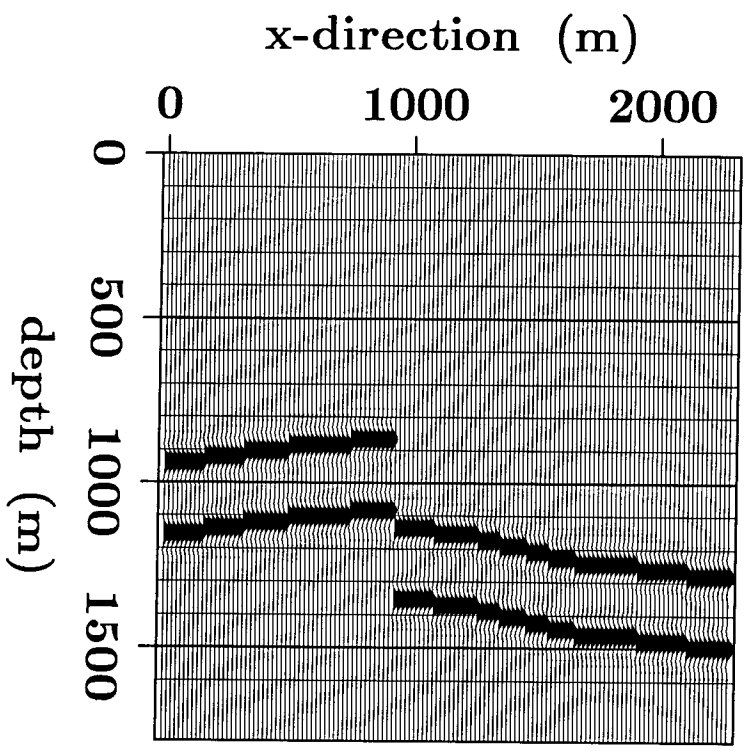

FIG. 1. Slice of constant $y = 1\ 152$ meters through the reflectivity model, showing the reflectors.

Example

To demonstrate the method, a model 3-D subsurface was constructed, and nine shot profiles were modeled with a three dimensional finite-difference modeling program. Figures 1-3 show a set of slices through a filtered version of the model to show the reflector locations. The original model consisted of 128 by 128 by 100 grid points in x, y, z respectively. The grid spacing was 18 meters in x, y, z. Each of the nine profiles was recorded on the grid of 128 by 128 receivers (in x, y) on the surface of the model. The time sample interval was 2 milliseconds, 650 time steps were recorded for each profile. The memory storage required for the velocity model and the wave field during the modeling calculations was 29 Megabytes. The modeling computations required 70 cpu-minutes per profile. Figures 4 and 5 show two lines of the recorded wave field for a shot located at receiver 64 (in x), line 64 (in y). The constant y slices are called lines and the constant x slices are constant receiver numbers. Figure 4 shows line 64 of the recorded wave field; Figure 5 shows line 100 of the recorded wave field.

All nine profiles were migrated using the method just described. The migrations required 30 Megabytes of core memory to hold the back-propagated wave field and the shot traveltimes and amplitudes. Each profile migration required 80 cpu-minutes. Figure 6-8 show slices of constant y through the migrated image. Figure 6 shows 3-D prestack migrated line 44; Figure 7 shows 3-D prestack migrated line 64; and Figure 8 shows 3-D prestack migrated line 84. Figures 9 and 10 show two lines of constant x. Figure 9 shows a slice of the 3-D prestack migrated image at receiver number 44; Figure 10 shows a slice at receiver

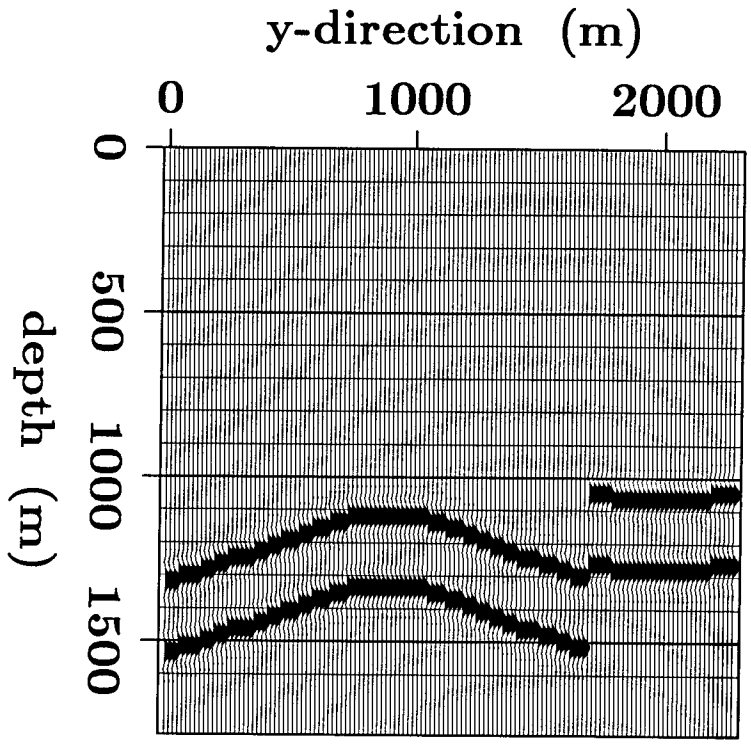

FIG. 2. Slice of constant $x = 1\ 152$ meters through the reflectivity model, showing the reflectors.

number 64. Figures 11 and 12 are slices through the image in constant depth. Figure 11 shows a slice at a depth of 882 meters; Figure 12 shows a slice at a depth of 1 116 meters. The image is confined to the central portion of the model because the nine shots were within 20 points in any direction from the center of the model. There are some artifacts present due to the small number of shots, but the image of the reflectors is accurate.

It is possible to migrate larger datasets using larger velocity models by separating the velocity model into several horizontal layers. Waves are propagated through each layer and the portion of the wave field that goes through the bottom of a layer is saved and introduced into the next layer. The calculations for each layer take place sequentially, consuming less core memory than if the entire model was held in core and the computation carried out in one run. This approach is particularly important for 3-D post-stack migration where most of the wave field travels downward. The method presented easily simplifies to the 3-D post-stack reverse-time migration method.

KIRCHHOFF INTEGRAL PRESTACK MIGRATION

Prestack migration of a 3-D survey with data collected along single lines requires imaging many shots and many lines. Each shot, although only collected along a line, is downward-continued in 3-D and imaged. Equation (2) is the 3-D downward-continuation equation for data collected on the surface (Schneider, 1978). $\tau(r; x, y, z)$ is the traveltime of the WKB Green's function for a wave traveling from the given image point x, y, z to the receiver point

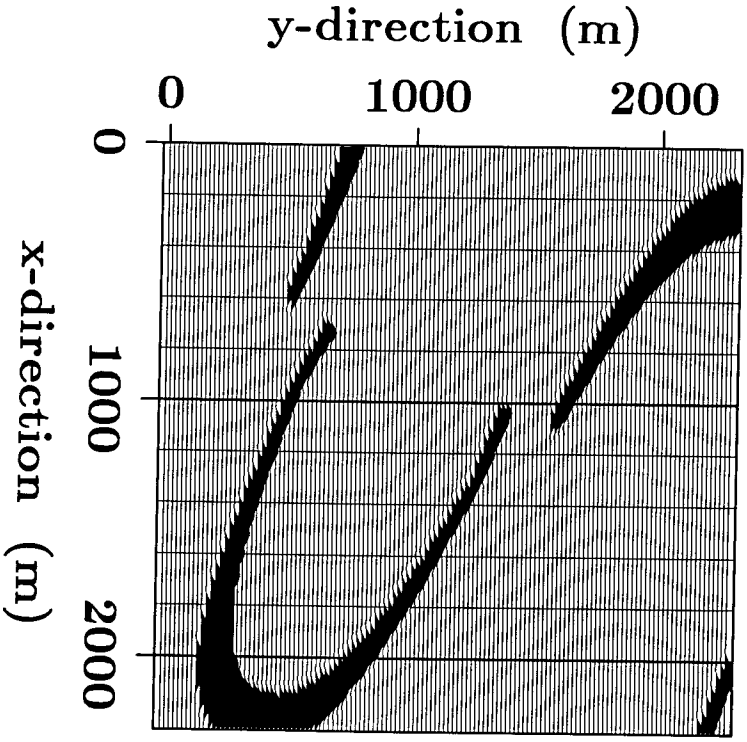

FIG. 3. Slice of constant $z = 1\ 200$ meters through the reflectivity model, showing the reflectors.

r. $A(r;x,y,z)$ is the amplitude of this WKB Green's function. U_{dwcnt} is the downward continued wave field as a function of x,y,z,t. $U_{recorded}$ is the wave field recorded on the surface. Note that this wave field extrapolation does not account for multiples so it is useful in the context of migrating primary reflections only.

$$U_{dwcnt}(x,y,z,t) = -\frac{1}{2\pi}\frac{\partial}{\partial z}\int_{receivers} A(r;x,y,z)\cdot U_{recorded}\left[r,s,t+\tau(r;x,y,z)\right]\ dr \qquad (2)$$

To image the downward-continued wave field, it is multiplied by the amplitude of the shot wave field at the arrival time of the shot wave field. $A(s;x,y,z)$ is the amplitude of the shot wave field and $\tau(s;x,y,z)$ is the traveltime of the shot wave field traveling from the shot location to the image point. These traveltimes and amplitudes are obtained using the same method described in the paper on fast prestack depth migration (Etgen, 1987) in this report.

Equation (3) is the prestack migration of a 3-D survey. N is a factor accounting for the fold of the data. The equation is general and will allow any shot/receiver geometry. The reason it is especially useful for marine 3-D surveys is that the sum over receivers for a given shot is only one-dimensional. For general geometries the sum would be two-dimensional.

$$\begin{aligned} U_{image}(x,y,z) \;=\; & -\frac{1}{2\pi N}\sum_{shots}\frac{\partial}{\partial z}\sum_{receivers} A(s;x,y,z)\cdot A(r;x,y,z)\cdot \\ & \cdot U_{recorded}\left[s,r,\tau(s;x,y,z)+\tau(r;x,y,z)\right]\cdot\Delta r \end{aligned} \qquad (3)$$

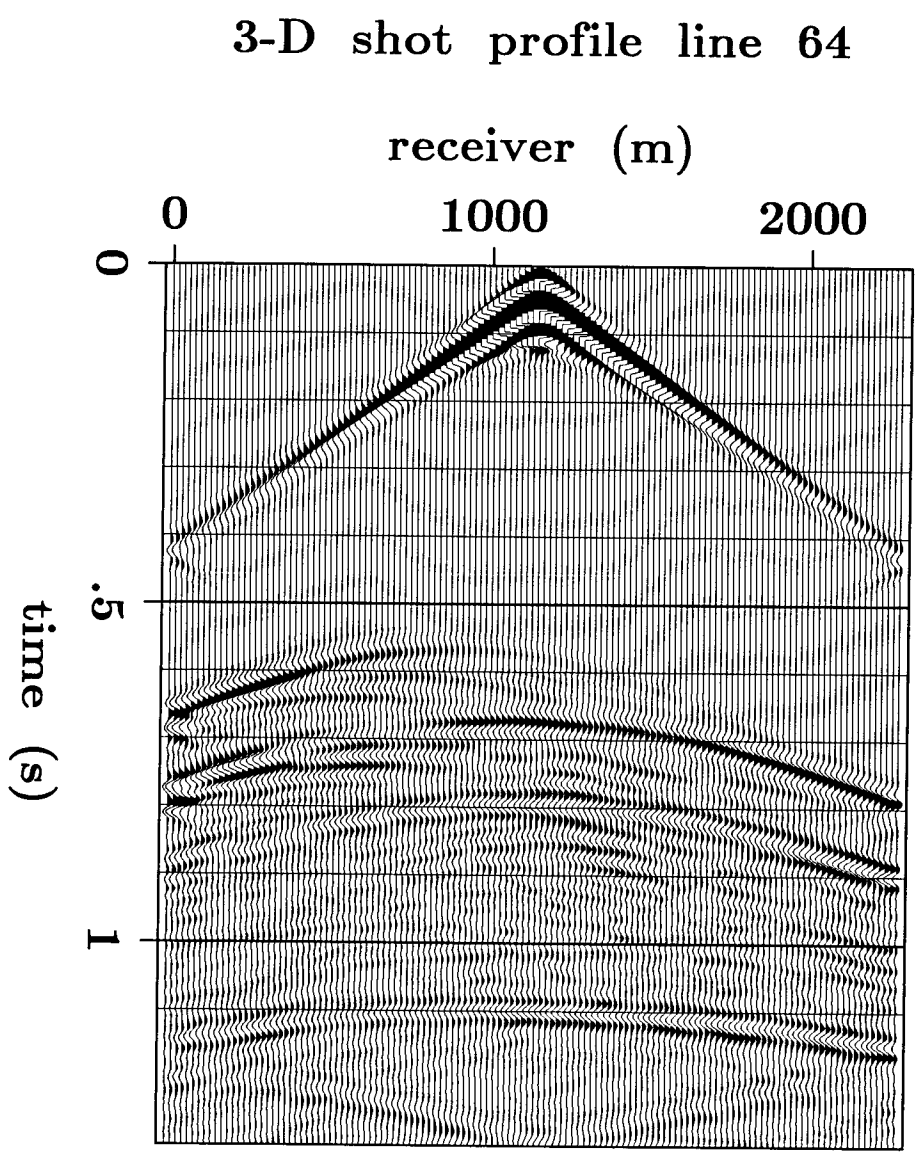

FIG. 4. Line 64 of recorded wave field for areal 3-D survey. The shot location was line 64 receiver number 64.

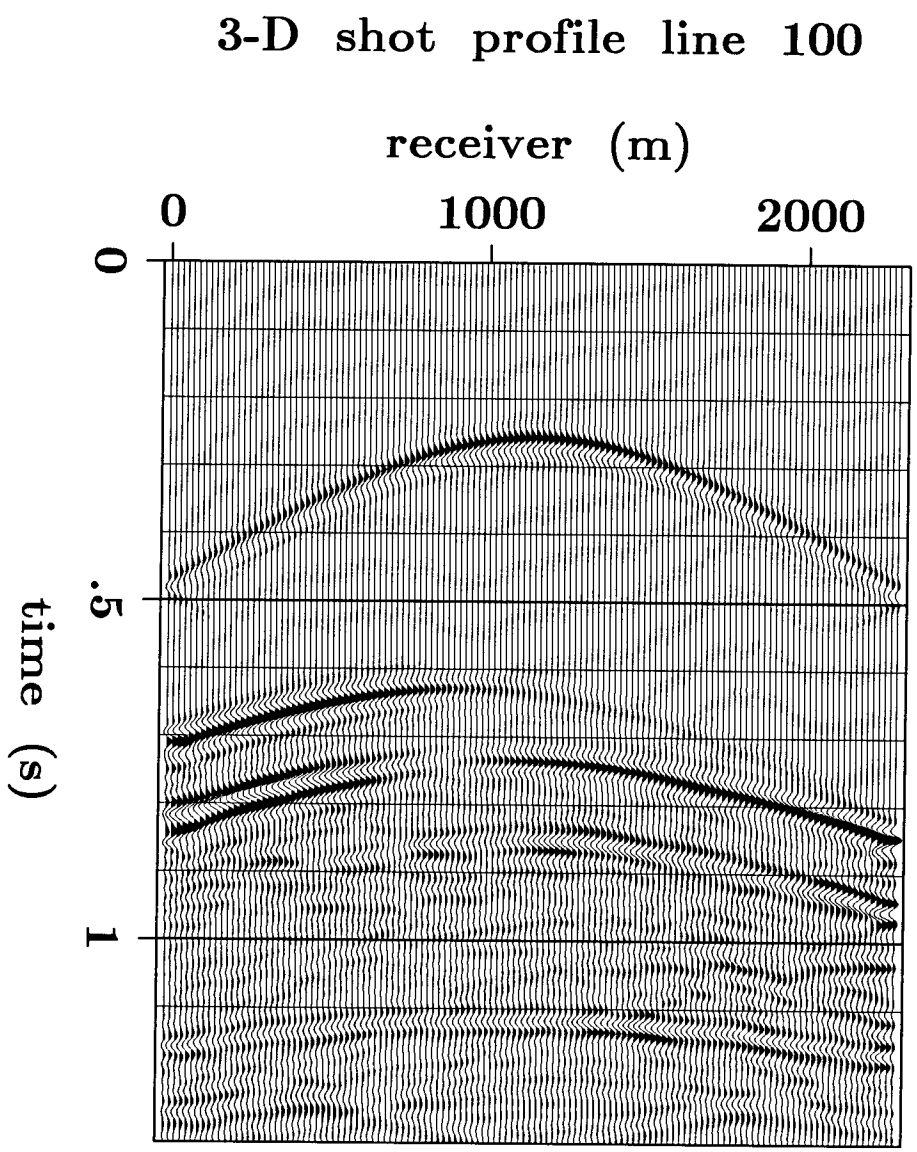

FIG. 5. Line 100 of recorded wave field for areal 3-D survey. The shot location was line 64 receiver number 64.

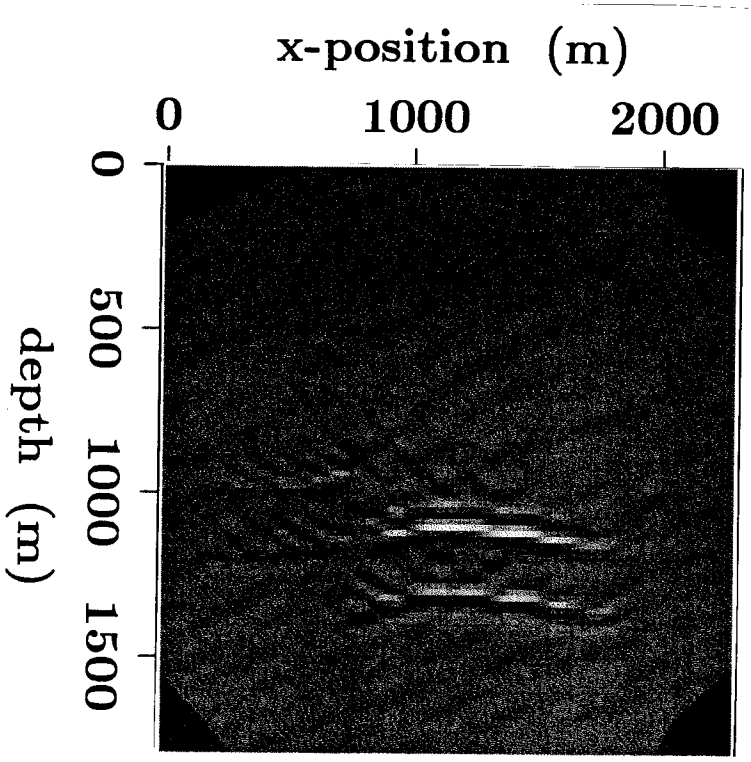

FIG. 6. Slice of constant y =792 meters (line 44) through image obtained using 3-D finite-difference reverse-time prestack migration method.

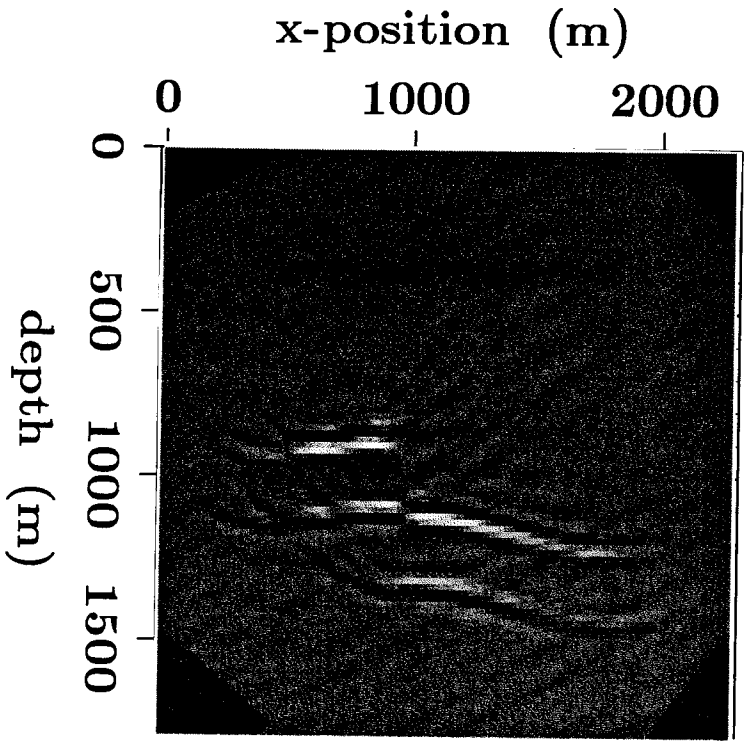

FIG. 7. Slice of constant y=1 152 meters (line 64) through image obtained using 3-D finite-difference reverse-time prestack migration method.

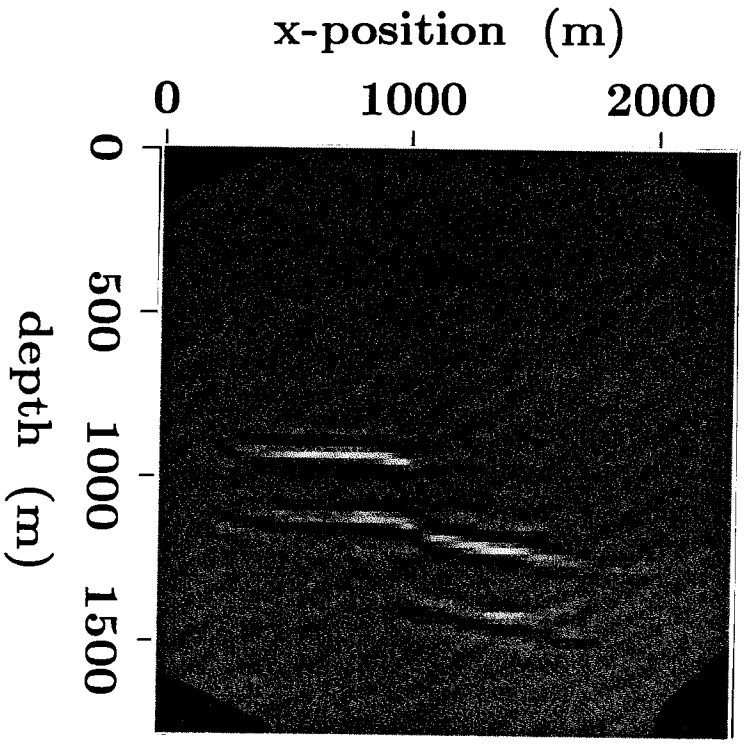

FIG. 8. Slice of constant y=1 332 meters (line 84) through image obtained using 3-D finite-difference reverse-time prestack migration method.

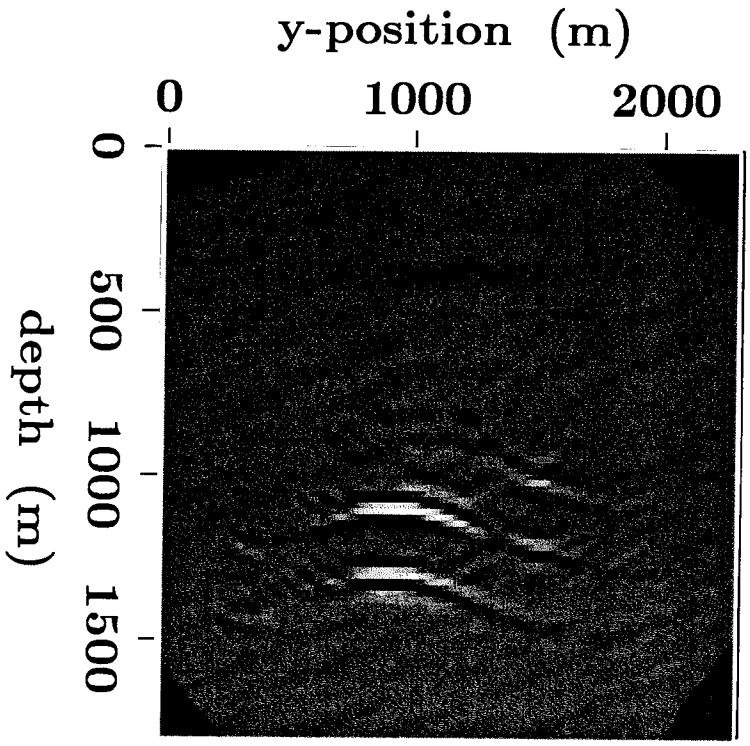

FIG. 9. Slice of constant x=1 044 meters (receiver 58) through image obtained using 3-D finite-difference reverse-time prestack migration method.

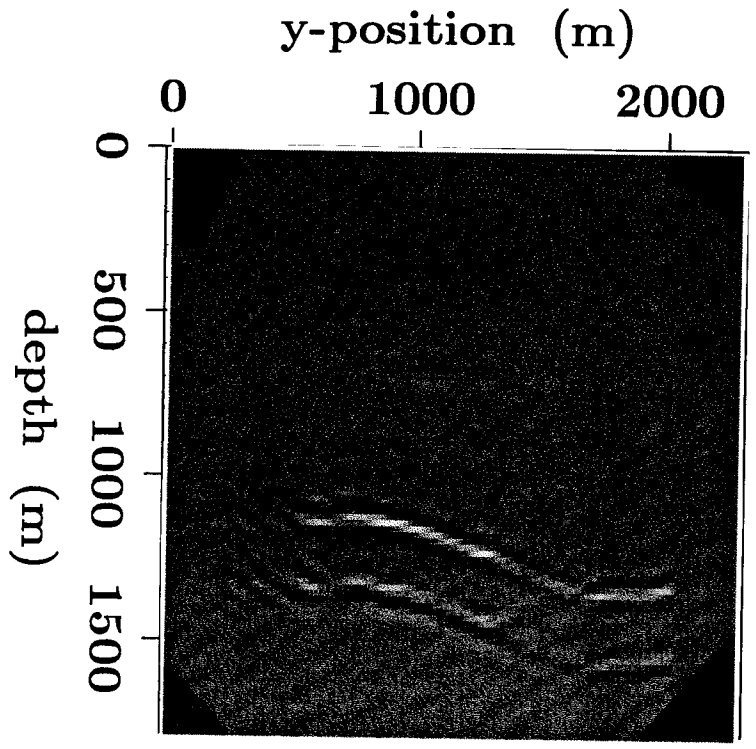

FIG. 10. Slice of constant x=1 512 meters (receiver 84) through image obtained using 3-D finite-difference reverse-time prestack migration method.

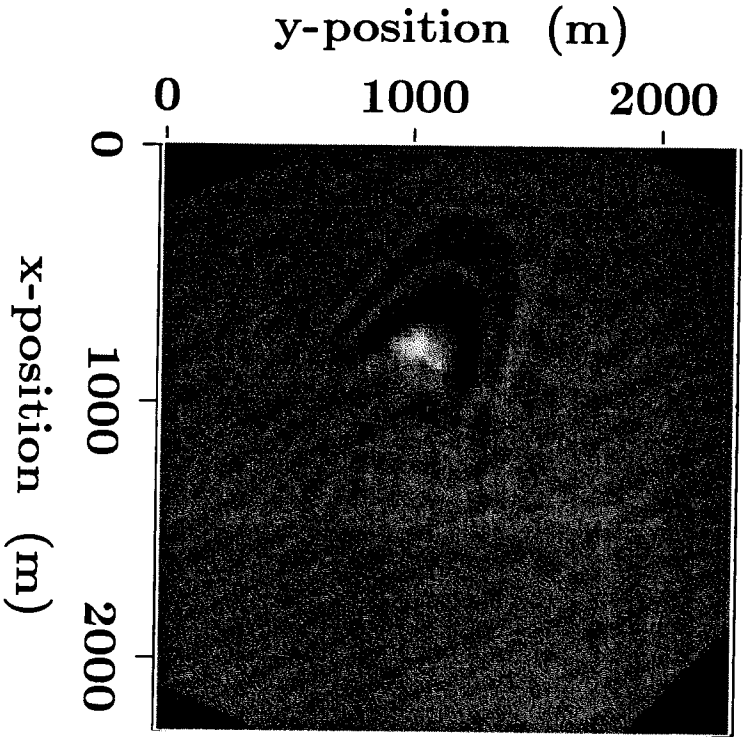

FIG. 11. Slice of constant z=882 meters through image obtained using 3-D finite-difference reverse-time prestack migration method.

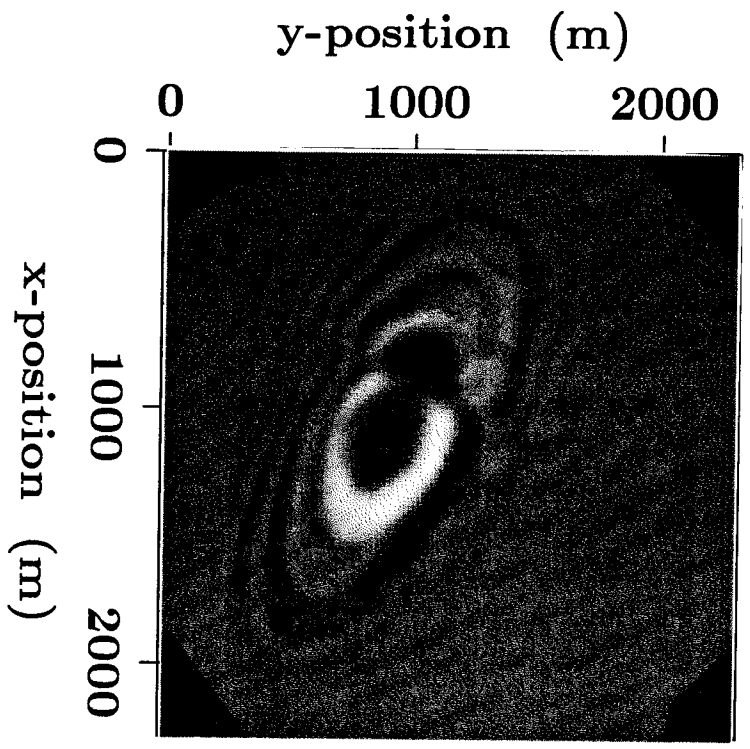

FIG. 12. Slice of constant z=1 116 meters through image obtained using 3-D finite-difference reverse-time prestack migration method.

Kirchhoff migration allows the use of a different imaging aperture in the cross-line direction than in the inline direction. This is useful when one axis is sampled differently than the other. When the cross-line spacing is sparse, spatial aliasing constraints require low dip migration operators. This is handled easily using the integral formulation by restricting the aperture of the sum (equation (3)) in the appropriate direction. Kirchhoff migration allows migrating data from an irregular input grid into a regular output grid. This is important for resolving problems like cable feathering or irregular line spacing.

The integral formulation allows a 3-D migration to be target oriented. A subset of the data can be used to provide an image for specific "target" zones in the model. The cost of the migration is only a function of the size of the image desired and the amount of data used to make the image. As noted before, when the data for a given profile is collected along a line, the cost of the sum over receivers is reduced to the cost of a one-dimensional sum. The finite-difference method does not enjoy a similar reduction of cost.

Example

A model dataset, similar to the one used for the finite-difference migration, was modeled with a Kirchhoff integral modeling algorithm. The original model was 128 by 128 by 100 grid points in x, y, z respectively; the grid spacing was 20 meters in each direction. The y direction is taken to be the cross-line direction and the x direction is the inline direction. Figure 13 shows a slice through a filtered version of the velocity model (constant y section, y=1 280 meters) to show the geometry of the reflectors. The general geometry of the reflectors is the same as the model used to test the finite-difference method, so no other

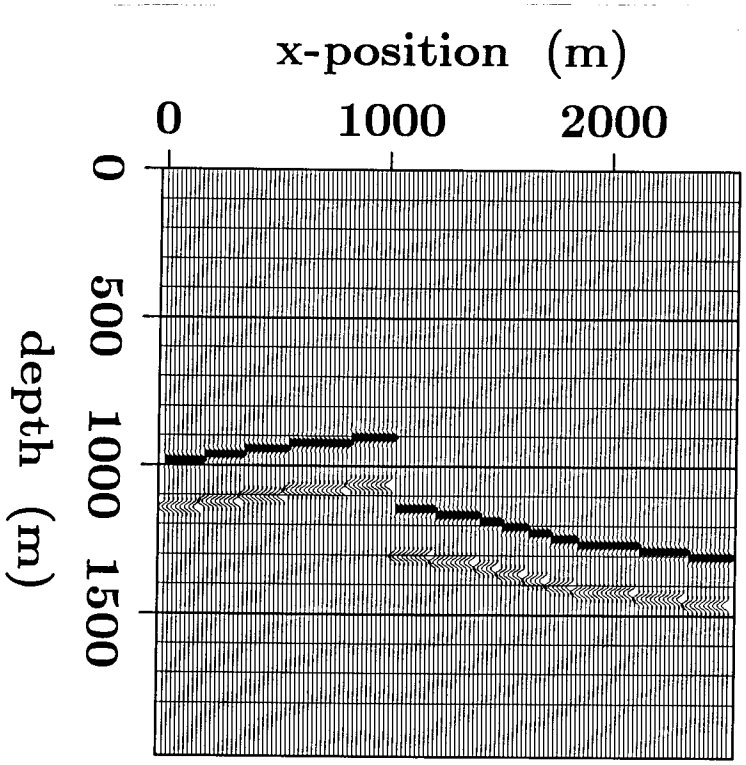

FIG. 13. Slice at y=1 280 meters through the reflectivity model used for 3-D Kirchhoff integral prestack migration test.

views of the model are shown.

The modeling operator allowed all dips to contribute to the model profiles. Fifty lines of data were collected with 40 meter spacing between the lines. The inline receiver spacing was 20 meters. On even numbered lines, 3 shot profiles were collected; on odd numbered lines, 4 shot profiles were collected, staggered from those on the even numbered lines. A total of 175 shot profiles were collected over the model. Figure 14 shows one shot profile from the 3-D dataset. The shot location was line 64, receiver number 54. The receivers were all along line 64.

The 175 model profiles were migrated using the Kirchhoff integral method described. Because of the sparse sampling in the y direction compared to the x direction, The migration operator was limited to approximately 30 degrees dip in the y direction. The operator was not limited in the x direction. As noted before, the image of one profile or one line of constant y does not contain sufficient information about the y direction to form an image of the subsurface. Therefore, the partial images, before all lines were migrated, were not examined. The 3-D prestack migration of each shot profile required 3 cpu-minutes. The migration of the entire survey required approximately 10 cpu-hours. Figures 15-17 show slices of constant y through the prestack migrated image obtained from all 175 profiles. Figure 15 is a slice at line 44; Figure 16 is a slice at line 64; and Figure 17 shows a slice at line 84. Figures 18 and 19 show slices through the prestack migrated image in constant x. Figure 18 shows a slice at receiver number 44; Figure 19 shows a slice at receiver number 58. Figures 20 and 21 show slices through the prestack migrated image at constant depth.

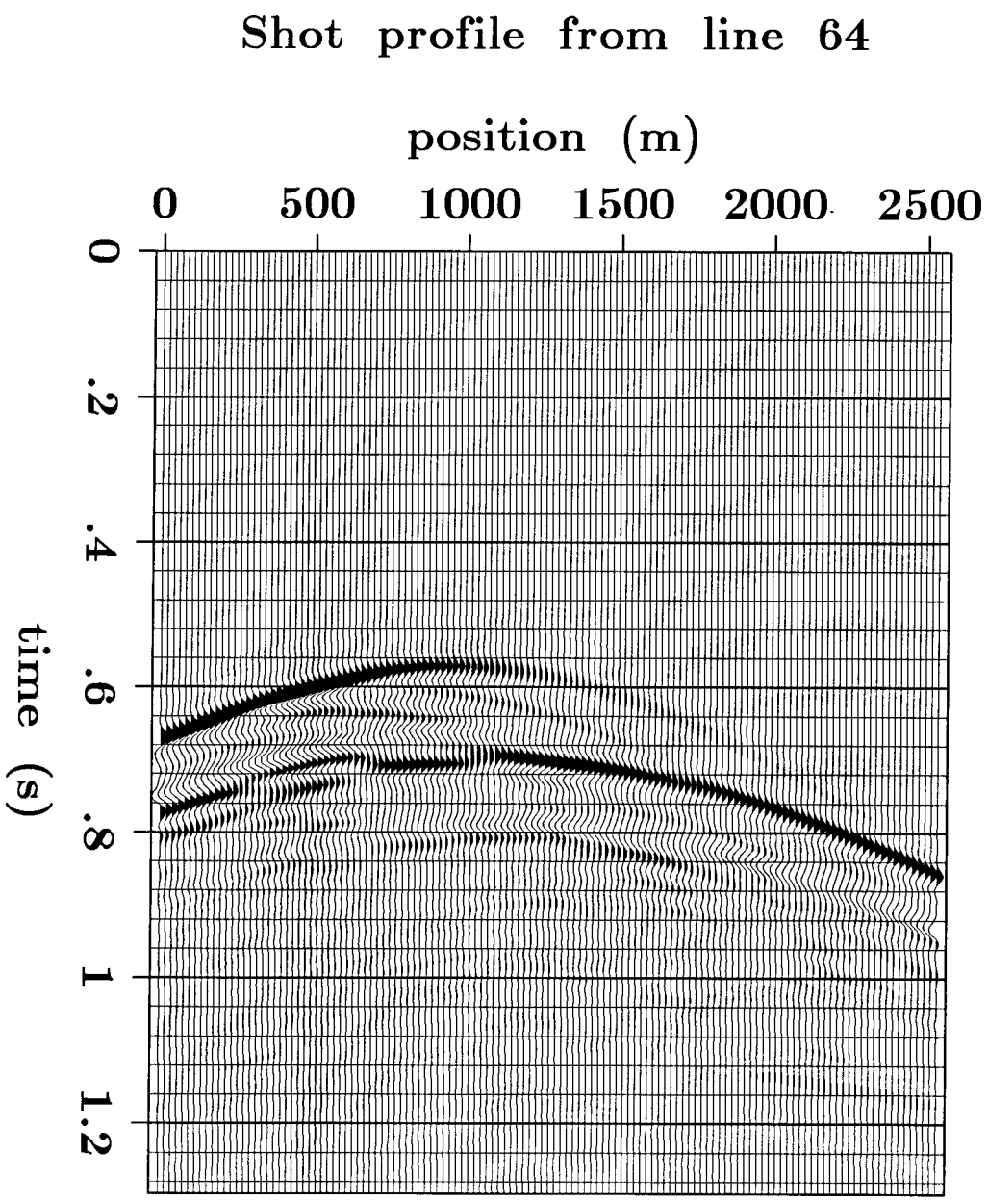

FIG. 14. Shot profile from model 3-D survey generated using a Kirchhoff integral modeling algorithm. the shot point is at line 64 receiver number 54.

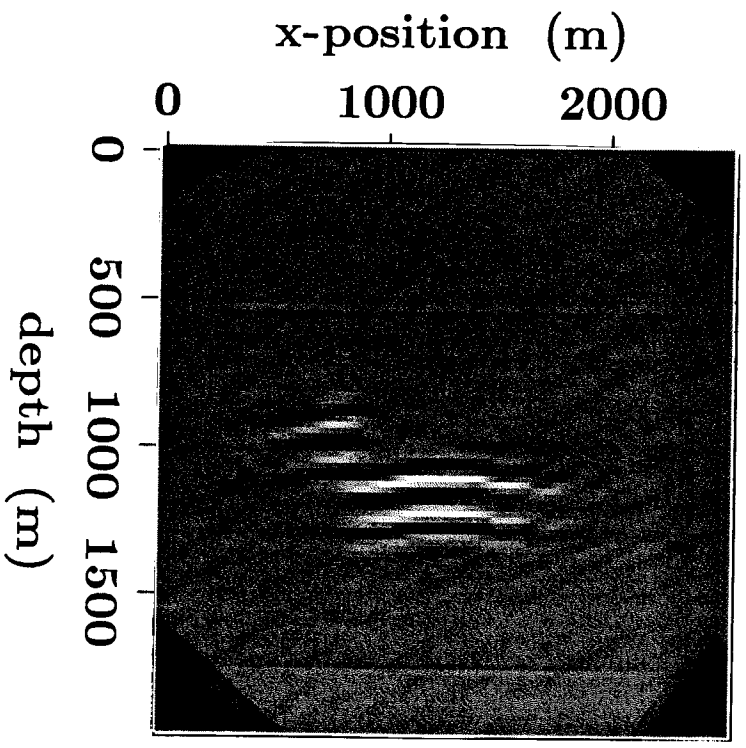

FIG. 15. Slice of constant y=880 meters (line 44) through image obtained using the Kirchhoff integral prestack migration method.

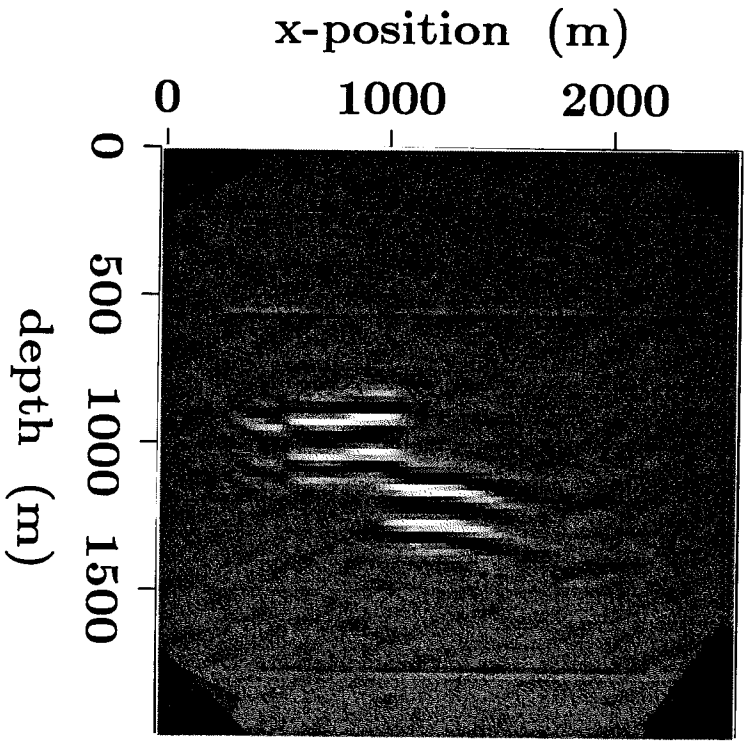

FIG. 16. Slice of constant y=1 280 meters (line 64) through image obtained using the Kirchhoff integral prestack migration method.

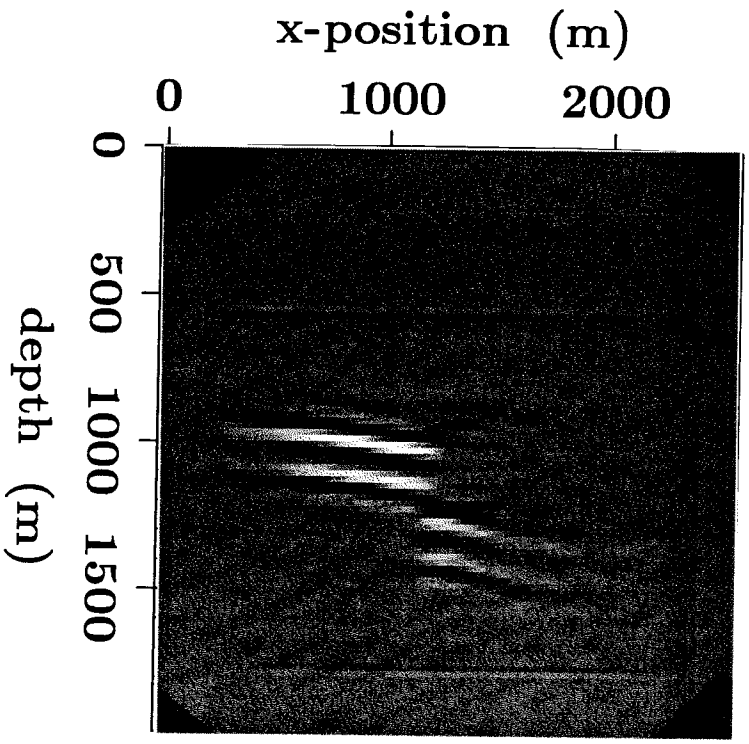

FIG. 17. Slice of constant y=1 680 meters (line 84) through image obtained using the Kirchhoff integral prestack migration method.

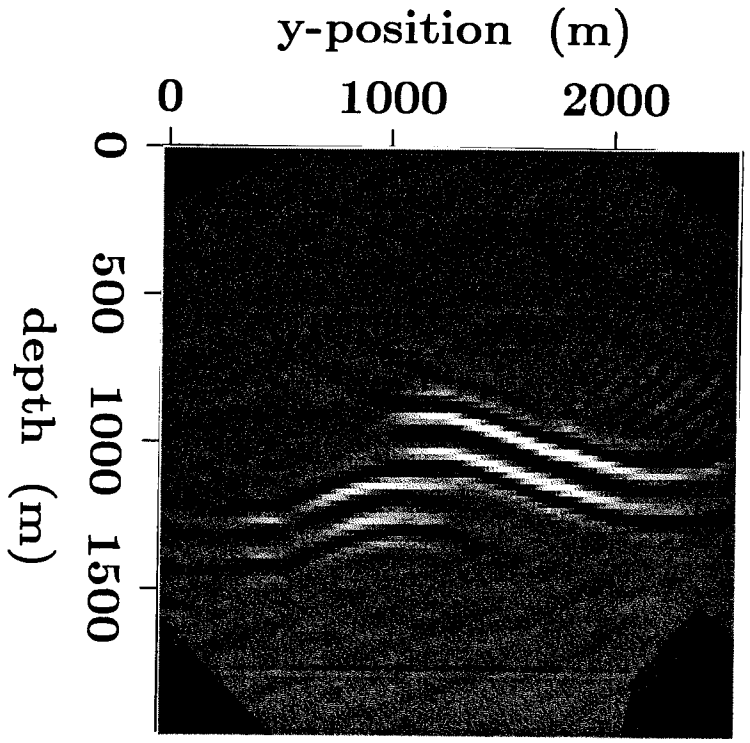

FIG. 18. Slice of constant x=960 meters (receiver 48) through image obtained using the Kirchhoff integral prestack migration method.

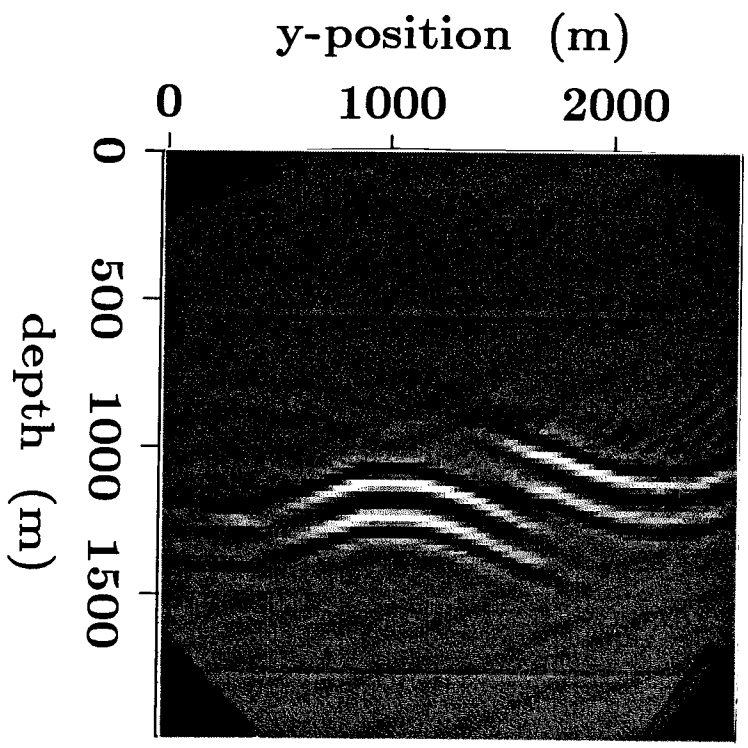

FIG. 19. Slice of constant x=1 200 meters (receiver 60) through image obtained using the Kirchhoff integral prestack migration method.

Figure 20 shows a slice at a depth of 900 meters; Figure 21 shows a slice at a depth of 1 100 meters. In the images shown, there are some artifacts present due to the small aperture of the survey, and the limited number of shots migrated, but the reflectors are correctly positioned.

CONCLUSIONS

The two methods presented accurately image 3-D shot profiles. The finite-difference method is suited for data collected with receivers in both x and y directions for each shot profile, such as a high-resolution 3-D land survey. Kirchhoff migration accurately images shot profiles in 3-D even if the data are collected along single lines. Although no tests were run, the methods will migrate 3-D stacked data if appropriately altered. Each method is capable of prestack migrating small 3-D surveys in about 10 cpu-hours. The finite-difference method requires a computer with large core-memory because of the many grid points present in the subsurface model. The Kirchhoff integral method is more expensive, but requires less memory and is "target oriented". The finite-difference method is preferable to the Kirchhoff integral method when the data are well sampled in both directions and on a nearly even grid such as in a high-resolution 3-D land survey. The Kirchhoff integral method is preferable to the finite-difference reverse-time method when the grid of receivers for a given shot profile is irregular, or only one-dimensional. The Kirchhoff integral method can handle cable feathering and irregular line spacing common to 3-D marine surveys.

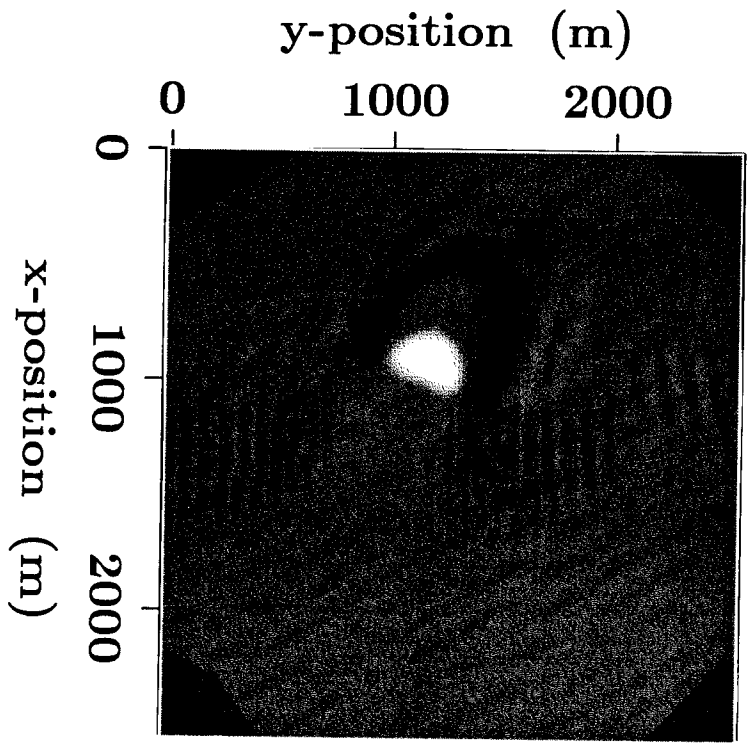

FIG. 20. Slice of constant z=900 meters through image obtained using the Kirchhoff integral prestack migration method.

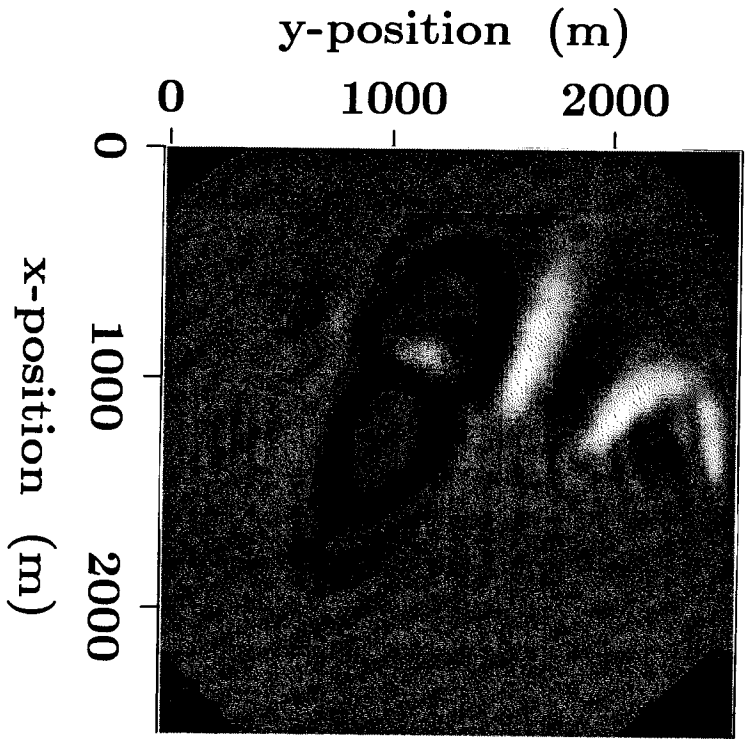

FIG. 21. Slice of constant z=1 100 meters through image obtained using the Kirchhoff integral prestack migration method.

ACKNOWLEDGMENTS

Thanks to Steve Cole and Joe Dellinger for writing **Ta2vplot**, the program that made the variable intensity plots in this report.

REFERENCES

Bleistein, N., Cohen, J.K., and Hagin, F.G., 1987, Two and one-half dimensional Born inversion with an arbitrary reference: Geophysics, **52**, 26-36.

Deregowski, S.M., 1985, Prestack depth migration by the boundary integral method: Presented at the 55th annual International SEG meeting October, 1985, in Washington D.C.

Etgen, J.T., 1986, Prestack reverse time migration of shot profiles: SEP-50, 151-169.

Etgen, J.T., 1987, Fast prestack depth migration using a Kirchhoff integral method: This report.

Gray, S.H., 1986, Efficient traveltime calculations for Kirchhoff migration: Geophysics, **51**, 1685-1688.

Schneider, W.A., 1978, Integral formulation for migration in two and three dimensions: Geophysics, **43**, 49-76.